Catalysis Letters 29 (1994) 145–158

Limitations of surface analytical techniques for determining the surface composition of bimetallic particles ☆

Allen G. Sault

Fuel Science Department 6211, Sandia National Laboratories, MS 0710, Albuquerque, NM 87185, USA

Received 13 May 1994; accepted 15 August 1994

Calculations of expected X-ray photoelectron spectroscopy intensity ratios for both homogeneous and segregated bimetallic particles demonstrate that a minimum particle size exists, below which reliable differentiation between homogeneous alloy particles and particles in which one component has segregated to the surface cannot be made. This minimum particle size varies between 3 and 8 nm depending on the specific metal combination in question. In cases of partial segregation of one component, the minimum particle size is even larger. The implications of these results for the study of surface segregation in supported bimetallic catalyst particles are discussed.

Keywords: bimetallic particles; bimetallic catalysts; X-ray photoelectron spectroscopy; Auger electron spectroscopy

1. Introduction

Bimetallic particles find important applications in heterogeneous catalysis [1–3]. A major consideration in the performance of these particles is the surface composition. Simple arguments regarding miscibility, heats of segregation and entropy change upon segregation [4], and heats of sublimation [1], suggest that preferential segregation of one component to the surface of bimetallic particles is the rule rather than the exception. Surface sensitive techniques such as X-ray photoelectron spectroscopy (XPS) and Auger electron spectroscopy (AES) have therefore been applied to the analysis of supported bimetallic particles in an attempt to determine the surface composition of particles with known overall composition [5–17]. Intuitively, it is obvious that these methods must fail below a certain critical particle size, when the attenuation lengths (AL) of the photoelectrons or Auger electrons

☆ This work was performed at Sandia National Laboratories for the US Department of Energy under contract DE-AC04-94AL85000.

become comparable to the particle diameter and essentially every photoelectron or Auger electron generated in the particle is detected regardless of location within the particle. Furthermore, for very small particles (<2 nm), a majority of the total atoms in the particle reside on the surface, and the concept of surface segregation becomes meaningless. In this paper, a theoretical method is presented, based on established quantitative methods for XPS, that calculates the change in the relative XPS signals from two metals in a bimetallic particle upon transformation from a homogeneous particle to a particle in which one component has segregated to the surface. Plotting this change as a function of particle size allows determination of the minimum particle size below which XPS cannot distinguish between a homogeneous alloy and a segregated particle. Results are presented for four different metal pairs in order to cover the entire range of expected behaviors. Depending on the specific metal pair in question, the minimum particle size varied from 3 to 8 nm. Since this size range coincides with the desired particle size for many catalytic applications, these results provide a basis for evaluating the utility of XPS and AES for determining the surface composition of bimetallic catalysts.

2. Methods

Four metal pairs are analyzed which differ in the AL's of the photoelectrons generated from Mg Kα radiation: (1) Cu on Ni (short AL on short AL); (2) Cu on Pd (short AL on long AL); (3) Pd on Cu (long AL on short AL); and (4) Pd on Ag (long Al on long AL). For the purposes of this discussion, AL's less than 0.9 nm are considered short, while those greater than 1.4 nm are considered long. The pairs are chosen to illustrate the types of behavior that can be expected, rather than to represent actual systems. For each pair, particle diameters (d) ranging from 1 to 64 nm, and mole fractions ranging from 0.1 to 0.9 are analyzed. For each pair, the XPS intensity ratios are calculated for both homogeneous alloy particles and particles with complete segregation of one metal to the surface. These two ratios are then compared to determine the minimum particle size necessary to allow experimental discrimination between the two cases.

All calculations assume a cubic particle shape for simplicity and use a layer by layer approach to calculate the expected XPS signals. In order to make this calculation, the signal from a single pure layer of a given metal must first be known. This signal is calculated from the bulk metal signal using the equation

$$I_{\mathrm{M}}^{\infty} = I_0 \sum_{n=1}^{\infty} \exp[-(n-1)a_{\mathrm{M}}/\lambda_{\mathrm{M}}], \tag{1}$$

where I_{M}^{∞} is the signal from a semi-infinite sample of metal M, I_0 is the signal from a single layer, a_{M} is the layer spacing in the bulk metal, and λ_{M} is the AL of the metal photoelectron. The photoelectron exit angle is assumed to be in the direction of the surface normal, an assumption which is equally valid for any experimental

geometry since the orientation of nanometer scale particles within an experimental sample is likely to be random. Performing the summation in (1) gives

$$I_0/I_M^\infty = 1 - \exp(-a_M/\lambda_M)\,. \tag{2}$$

Within a bimetallic particle, the signal from a given layer, I_0^P, is decreased because not all of the atoms are of the same element. Additionally, the number of atoms per unit area in a bimetallic layer ($1/a_P^2$) is potentially different from that of the bulk metals. Therefore the signal from a single layer in a bimetallic particle is given by

$$I_0^P/I_M^\infty \propto X_M(a_M/a_P)^2[1 - \exp(-a_M/\lambda_M)]\,, \tag{3}$$

where X_M is the mole fraction of metal M in the layer, and a_P is the layer spacing in the bimetallic particle. The proportionality arises because the particle layer does not extend infinitely in all directions as assumed in the derivation of (2). Further attenuation of the single layer signal by overlying layers in the particle necessitates the addition of an exponential attenuation term, i.e.

$$I_0^P/I_M^\infty \propto X_M(a_M/a_P)^2[1 - \exp(-a_M/\lambda_M)]\exp[-(n-1)a_P/\lambda_P]\,, \tag{4}$$

where $(n-1)$ is the number of layers above the nth layer and λ_P is the AL of the metal photoelectrons in the bimetallic particle, which can differ from λ_M through the dependence of AL on layer spacing [18].

Summing the values of I_0^P/I_M^∞ for both metals in all layers of the particle allows the sensitivity corrected signal intensities (I_M^P/I_M^∞) of the two metals to be calculated. Since the proportionality factor in eq. (4) is the same for both metals, taking the ratio of the signals from the two metals gives $(I_{M_s}^P/I_{M_s}^\infty)/(I_{M_c}^P/I_{M_c}^\infty)$ exactly, where M_s is the segregating metal and M_c is the core metal. No consideration of angular asymmetry in photoelectron emission is made in the analysis, amounting to the assumption that the angle between the incident X-rays and the analyzer axis is the "magic angle" of 54°44′ [19] at which the ratios of the photo-ionization cross sections are the same as if photoelectrons were collected over a 4π solid angle, or alternatively that angular effects are accounted for in the values of I_M^∞.

Although the calculations are performed for XPS, the analysis also applies to Auger electron spectroscopy (AES) provided backscattering is taken into account [20]. Since backscattering factors are only a weak function of atomic number for the transition metals [21], the XPS calculations should be quantitatively applicable to AES for metal pairs that have similar atomic numbers, but only qualitatively applicable for metal pairs that differ significantly in atomic number. The details of the calculations and summations differ slightly for homogeneous and segregated particles.

2.1. HOMOGENEOUS PARTICLES

For homogeneous bimetallic particles, the fractional occupancy of one metal in

any given layer is simply the mole fraction of the metal present in the particle. Layer spacing, a_P, is assumed to be a composition weighted average of the layer spacings of the pure elements, a_M, which are derived from the atomic weights and elemental densities according to

$$a_M^3 = \frac{W_M}{\rho_M A}, \tag{5}$$

where A is Avagadro's number, ρ_M is the metal density and W_M is the atomic weight of metal M. AL's for the individual components are taken from Seah and Dench [18] according to

$$\lambda_M = (0.41)a_M^{1.5}E_M^{0.5} \quad \text{and} \quad \lambda_P = (0.41)a_P^{1.5}E_M^{0.5}, \tag{6}$$

where E_M is the kinetic energy of the photoelectron generated by metal M. Table 1 lists values of a_P and λ_P for the various metal pairs under consideration as well as photoelectron kinetic energies. Values of a_M and λ_M for the pure metals are given in table 2.

2.2. SEGREGATED PARTICLES

For segregated particles the first step in the calculation involves determining the coverage of the segregated metal on the particle surface. This is accomplished by comparing the number of surface atoms on a particle (N_{surf}) to the number of

Table 1
Theoretical parameters used in homogeneous particle calculations

Metal pair (M_1/M_2)	X_{M_1} [a]	a_P [b] (nm)	KE(M_1) [c] (eV)	KE(M_2) [c] (eV)	λ_1 [d] (nm)	λ_2 [d] (nm)
Cu/Ni	0.1	0.223	321	401	0.77	0.86
Cu/Ni	0.5	0.225	321	401	0.78	0.88
Cu/Ni	0.9	0.227	321	401	0.79	0.88
Cu/Pd	0.1	0.243	321	919	0.88	1.49
Cu/Pd	0.5	0.237	321	919	0.84	1.43
Cu/Pd	0.9	0.230	321	919	0.81	1.37
Pd/Cu	0.1	0.230	919	321	1.37	0.81
Pd/Cu	0.5	0.237	919	321	1.43	0.84
Pd/Cu	0.9	0.243	919	321	1.49	0.88
Pd/Ag	0.1	0.257	919	885	1.62	1.59
Pd/Ag	0.5	0.252	919	885	1.57	1.54
Pd/Ag	0.9	0.246	919	885	1.52	1.49

[a] Mole fraction of M_1.
[b] Estimated interlayer spacing in homogeneous bimetallic particles.
[c] Kinetic energy of photoelectrons generated by M_1 and M_2 ($2p_{3/2}$ for Cu and Ni, $3d_{5/2}$ for Ag and Pd).
[d] AL of photoelectrons generated from the two metals by Mg Kα radiation in the homogeneous bimetallic environment (from Seah and Dench [18]). These values are labeled λ_P in the text.

Table 2
Theoretical parameters used in segregated particle calculations

	M_s on M_c			
	Cu on Ni	Cu on Pd	Pd on Cu	Pd on Ag
a_{M_s} [a] (nm)	0.228	0.228	0.245	0.245
a_{M_c} [a] (nm)	0.222	0.245	0.228	0.258
λ_{M_s,M_s} [b] (nm)	0.80	0.80	1.51	1.51
λ_{M_s,M_c} [b] (nm)	0.77	0.89	1.35	1.63
λ_{M_c,M_s} [b] (nm)	0.89	1.35	0.89	1.48
λ_{M_c,M_c} [b] (nm)	0.86	1.51	0.80	1.60

[a] a_M is the layer spacing in metal M.
[b] λ_{M_i,M_j} is the AL of M_i photoelectrons in M_j. The λ_{M_i,M_i} values are also used in the calculations for homogeneous particles, and are labeled λ_M in the text.

atoms of segregating metal (N_{seg}) in the particle. If N_{surf} exceeds N_{seg}, then N_{seg}/N_{surf} gives the coverage of the segregating metal. If N_{seg} exceeds N_{surf}, then a complete layer of segregating metal will be formed and the calculation must be repeated for the second layer in the particle. In general, a certain number of complete layers of the segregating metal will be formed over a mixed layer containing both metals.

After determining the coverage of the segregating metal, the XPS signals can be calculated taking care to use the proper AL's, a_P values, and mole fractions for each metal in each layer. For instance, for core metal atoms the photoelectrons first pass through a number of layers of the core metal, then through the mixed layer, and finally through any complete layers of segregating metal that may be present. Since the AL depends weakly on layer spacing [18], the AL will vary slightly as the electron passes through each region of the particle. For the core metal, setting a_P equal to a_M is a reasonable assumption. For the overlayer metal, however, the situation is not so clear. Experimentally, studies of metal overlayer deposition indicate that pseudomorphic growth generally occurs for the first one to two layers [22]; i.e., the lattice spacing of the segregated metal parallel to the surface adopts the value of the core metal. Based on this result, the value of a_P for the overlayer metal might therefore be set equal to the value for the core metal. In the direction perpendicular to the surface, however, the layer spacing can be either compressed or expanded relative to the bulk, depending on whether pseudomorphic growth results in compression or extension of the overlayer metal lattice spacing parallel to the surface. Furthermore, the assumption of pseudomorphic growth breaks down after the first one to two layers, and the overlayer structure relaxes to the bulk structure of the overlayer metal [22]. Fortunately, uncertainty in a_P has little effect on the calculation for two reasons. First, values of a_M do not vary greatly for the transition metals under consideration (see table 2). In fact, the uncertainty introduced by assuming a value of a_P in eq. (6) is less than the uncertainty introduced by the use of either general correlations such as eq. (6), or experimental AL or inelastic

mean free path (IMFP) measurements [18,23–25]. Second, a_P appears in the calculations only in the exponential attenuation term and the $(a_M/a_P)^2$ term in (4), and in the calculation of λ_P. Since λ_P varies as $a_P^{1.5}$, division of a_P by λ_P results in an $a_P^{-0.5}$ dependence of the exponent in (4). This weak dependence, coupled with the small variations in a_M among the various metals, ensures that the exponential term is relatively insensitive to a_P. The $(a_M/a_P)^2$ term is a serious consideration for large particles where the segregating metal forms many layers and the assumption of pseudomorphic growth breaks down. As will be seen below, however, the most interesting behavior occurs for small particles, where the coverage of overlayer metal is lowest and the assumption of pseudomorphic growth is most likely to be valid. In fact, trial calculations using different assumptions for a_P result in variations of only a few percent in the values of $(I^P_{M_s}/I^\infty_{M_s})/(I^P_{M_c}/I^\infty_{M_c})$, demonstrating that assumptions regarding a_P are not critical to the conclusions presented here.

For calculations of AL's, a_P is therefore taken to be equal to the bulk a_M values for both the core metal and the segregated overlayers, while a_P for the mixed layer is set equal to the core metal value. For calculations of attenuation, a_P for the core metal is set equal to the bulk value for the core metal. For the segregated metal, the assumed value depends on the path of the photoelectrons. For photoelectrons that travel through the top or bottom segregated layers, a_P is set equal to a_M for the segregating metal. For photoelectrons that travel through the side segregated layers of the particle, a_P is set equal to a_M of the *core* metal, in accordance with the assumption of pseudomorphic growth. The assumed values of a_M and λ_M for the various metal pair combinations are given in table 2.

3. Results and discussion

Tables 3 and 4 list the calculated XPS intensity ratios for selected homogeneous $(R_h = (I^P_{M_s}/I^\infty_{M_s})_h/(I^P_{M_c}/I^\infty_{M_c})_h)$ and segregated particles $(R_s = (I^P_{M_s}/I^\infty_{M_s})_s/(I^P_{M_c}/$

Table 3
Calculated XPS intensity ratios for homogeneous particles

d (nm)	M_s/M_c					
	Cu/Pd[a]			Pd/Ag[a]		
	$X_{Cu} = 0.1$	$X_{Cu} = 0.5$	$X_{Cu} = 0.9$	$X_{Pd} = 0.1$	$X_{Pd} = 0.5$	$X_{Pd} = 0.9$
1.0	0.138	1.24	11.2	0.101	0.91	8.20
1.9	0.121	1.09	9.79	0.102	0.92	8.23
3.9	0.106	0.95	8.57	0.102	0.92	8.28
7.8	0.100	0.90	8.11	0.102	0.92	8.31
15.6	0.099	0.89	8.07	0.102	0.92	8.31
31.1	0.099	0.89	8.07	0.102	0.92	8.31

[a] The reported values are for $R_h = (I^P_{M_s}/I^\infty_{M_s})_h/(I^P_{M_c}/I^\infty_{M_c})_h$.

Table 4
Calculated XPS intensity ratios for segregated particles

d (nm)	M_s/M_c					
	Cu/Pd[a]			Pd/Ag[a]		
	$X_{Cu} = 0.1$	$X_{Cu} = 0.5$	$X_{Cu} = 0.9$	$X_{Pd} = 0.1$	$X_{Pd} = 0.5$	$X_{Pd} = 0.9$
1.0	0.138	1.25	11.4	0.101	0.91	8.32
1.9	0.125	1.15	10.5	0.103	0.94	8.73
3.9	0.133	1.23	11.0	0.112	1.07	10.3
7.8	0.194	1.82	18.3	0.150	1.56	17.8
15.6	0.353	3.76	73.4	0.253	3.31	71.1
31.1	0.673	12.6	1317	0.481	11.8	1220

[a] The reported values are for $R_s = (I^P_{M_s}/I^\infty_{M_s})_s/(I^P_{M_c}/I^\infty_{M_c})_s$.

$I^\infty_{M_c})_s$), respectively. The particle sizes listed in these tables are only approximate since the independent variable in the calculations is the number of layers in the particle, and the values of the layer spacing vary slightly with the metal pair in question. This slight variation does not affect any conclusions drawn from this work.

For homogeneous particles, XPS ratios approach an asymptotic limit as particle size increases. These asymptotic values agree within 1% with the ratios calculated for bulk alloys by the method described by Briggs and Seah [20], providing confidence in the accuracy of the calculations presented here. For smaller particles, the variation of R_h depends on the metal pair in question. For the Pd/Ag (long AL/long AL) and Cu/Ni (short AL/short AL) systems, the AL's of the two photoelectrons are similar, so the XPS intensity ratio is fairly independent of particle size, even for small particles. In the Cu/Pd system, however, the AL of Cu $2p_{3/2}$ photoelectrons is much shorter than that of the Pd $3d_{5/2}$ photoelectrons. As a result, the copper signal reaches its asymptotic limit at a smaller particle size than the palladium signal, and the Cu $2p_{3/2}$/Pd $3d_{5/2}$ XPS ratio decreases with particle size.

In general, the calculated ratios for the segregated particles behave as expected. Because the surface to volume ratio of a cubic particle decreases as $1/d$, the surface coverage of the segregated metal (M_s) increases rapidly with particle size. This effect results in increasing enhancement of the signal from M_s, and increasing attenuation of the signal from the core metal (M_c) with particle size. As a result, all XPS intensity ratios for segregated particles grow rapidly with particle size. The rate of growth is greatest for particles with the highest concentration of segregating metal. This trend is due to the interplay of two different effects. As the mole fraction of M_s increases, the signal enhancement due to segregation decreases; for high mole fractions the surface already contains mostly M_s, so segregation cannot result in a large increase in the M_s XPS signal. Offsetting this effect is an increase in the attenuation of the core metal signal as the mole fraction of M_s increases. For low mole fractions of M_s, segregation results in only partial coverage of the outer-

most layer of the particle by the M_s, and as a result little attenuation of the M_c signal. For a high mole fraction of M_s, multiple layers of M_s are formed upon segregation, and a large attenuation of the M_c signal occurs. Based on the calculations, the increasing attenuation of the M_c signal with mole fraction of M_s overcomes the decreasing enhancement of the M_s signal, and the rate of change of the XPS ratios with particle size is greatest for particles with high mole fractions of M_s.

In the Cu/Pd system, anomalous behavior is observed at very low particle sizes, with the XPS ratio actually decreasing as the particle size increases from 1 to 2 nm for all mole fractions. This result can be explained by considering that for small particles, the M_c signal actually increases with particle size due to an increase in the number of layers of metal in the particles that contribute to the XPS signal. In the Cu/Pd system, this increase overcomes the increase in the M_s signal resulting from the increase in surface coverage with particle size. This effect can only be observed for particles with diameters smaller than or nearly equal to the AL of the core metal photoelectrons. For larger particles, the bottom layers of M_c in the particle make a negligible contribution to the XPS signal, so the M_c signal decreases with particle size due to attenuation by the M_s overlayers.

In order to determine the minimum particle size necessary to distinguish between a homogeneous alloy and a segregated particle by XPS, a comparison of the XPS ratios calculated for the two cases must be made. This comparison is made in figs. 1a–1d, where R_s/R_h is plotted as a function of particle size for the various metal pairs. For 1 nm particles, only $\sim$ 4 atomic layers are present, and nearly 90% of the atoms already reside on the surface of the particles. Thus, the concept of surface segregation is not applicable, and R_s/R_h is necessarily close to 1.0. As the particle size increases to 2.0 nm the fraction of atoms residing on the surface decreases to $\sim$ 60% and surface segregation begins to affect the XPS ratios, as shown by the increasing values of R_s/R_h in figs. 1a–1d. As expected, R_s/R_h continues to increase for particle sizes above 2 nm, although at different rates depending on the particular metal pair in question and the concentration of the segregating component. Clearly, for particle sizes greater than 10 nm differentiation between homogeneous particles and segregated particles is trivial since the XPS ratios differ by at least a factor of two in all but one case. For smaller particles the situation is not so clear. Based on AL and IMFP data presented by Seah and Dench [18] and others [23,24], it appears that generalized expressions can introduce uncertainties in AL values of at least 20–30% and possibly as high as a factor of two. Even experimental measurements of attenuation lengths are not accurate to greater than $\sim$ 20–30% [25]. Furthermore, XPS sensitivity factors (I_M^∞) must be accurately known in order to convert measured XPS intensities to $(I_{M_s}^P/I_{M_s}^\infty)/(I_{M_c}^P/I_{M_c}^\infty)$ for comparison with the calculations. Use of published sensitivity factors [26,27] can result in uncertainties on the order of 20–50% if the experimental conditions and the transmission characteristics of the spectrometer used to obtain the sensitivity factors differ from those of the experimental spectrometer [28]. Simulation of these uncertainties in the calculations indicates that the measured value of $(I_{M_s}^P/I_{M_s}^\infty)/(I_{M_c}^P/I_{M_c}^\infty)$ should be at

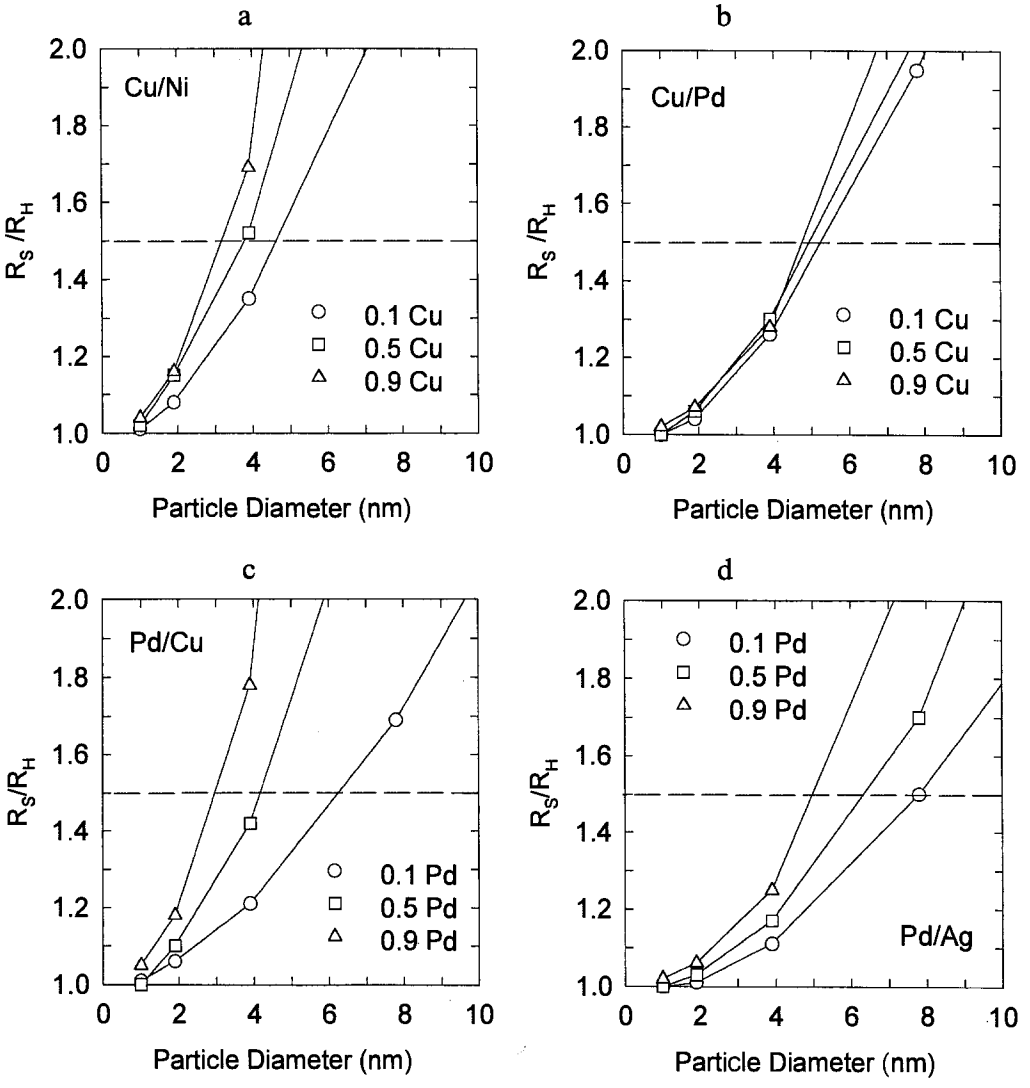

Fig. 1. R_s/R_h as a function of particle size for the various metal pairs. $R_h = (I^P_{M_s}/I^\infty_{M_s})_h/(I^P_{M_c}/I^\infty_{M_c})_h$; $R_s = (I^P_{M_s}/I^\infty_{M_s})_s/(I^P_{M_c}/I^\infty_{M_c})_s$. (a) Cu/Ni; (b) Cu/Pd; (c) Pd/Cu; (d) Pd/Ag.

least 50% greater than the calculated value of R_h before one can confidently state that surface segregation has occurred. The dotted lines in figs. 1a–1d indicate this point. The decision point could potentially be lowered below 50% by measurement of relative sensitivity factors for the pure metals on the same instrument that is to be used to analyze the unknown alloy particles. Quantification can also be improved by the use of appropriate standard materials for calibration, although it is doubtful that reproducible standards for segregated and homogeneous alloy particles could be established.

Based on the criteria for discriminating between homogeneous and segregated particles, fig. 1 shows that the minimum particle size for which segregation can be detected can be as low as 3 nm or as high as 8 nm, depending on the combination of metals chosen and the relative concentrations of the two metals in the particle. This conclusion is only valid in cases of complete segregation of one metallic component. In many cases, particularly when the two metals are partly or completely miscible, only partial segregation occurs. The extent of segregation depends on the miscibility of the metals [29], the heat of segregation, and the entropy change that accompanies segregation [5]. Note that metals which are immiscible in the bulk are sometimes found to be miscible in small particles [1]. For partial segregation the values of R_s/R_h will be smaller than presented in fig. 1 and the minimum particle size for which segregation can be discerned will be correspondingly greater.

For all metal pairs, the minimum particle size is smallest when the concentration of M_s is highest. This outcome is the result of the competing factors described above in the discussion of table 4. For a high concentration of M_s, the transition from a homogeneous particle to a segregated particle results in little change in the concentration of M_s on the surface, but a large decrease in the M_c signal due to attenuation by the overlying layers of M_s. For a low concentration of M_s, little attenuation of the M_c XPS signal occurs, but the surface concentration of the segregating metal increases greatly. Both situations result in values of R_s/R_h greater than one, but the attenuation of the M_c signal when the concentration of M_s is high is evidently stronger than the enhancement of the M_s signal when the M_s concentration is low.

A comparison of different metal pairs with the same concentrations of segregating metal is made in figs. 2a–2c. For a given segregating metal the minimum particle size is smallest when the core metal has a low AL. This result is physically understandable. Since the AL of photoelectrons from the segregating metal is only a weak function of the metal environment (through the $a^{1.5}$ term in eq. (6)), the enhancement of the M_s signal during the transition from a homogeneous particle to a segregated particle is relatively independent of the identity of the core metal. The loss in signal from the core metal due to attenuation by the segregated metal overlayers, however, depends strongly on the AL of the core metal photoelectrons. Thus, core metals with small AL's undergo more attenuation than core metals with large AL's, and the value of R_s/R_h rises faster with particle size for the core metals with small AL's. Similar arguments explain the change in the value of R_s/R_h when the AL of the segregating metal changes while the AL of the core metal stays the same (e.g., Cu/Pd versus Pd/Ag). In this case, attenuation of the M_c signal is relatively independent of the identity of M_s, while the enhancement of the signal from M_s is greatest for the segregating metal with the lower AL. The comparison of a system consisting of a low AL metal on a high AL metal (Cu/Pd) with a system of a high AL metal on a low AL metal (Pd/Cu) is not straightforward since the effects discussed above tend to offset each other. As a result, the relative magnitudes of R_s/R_h for Cu/Pd versus Pd/Cu change as the particle composition is var-

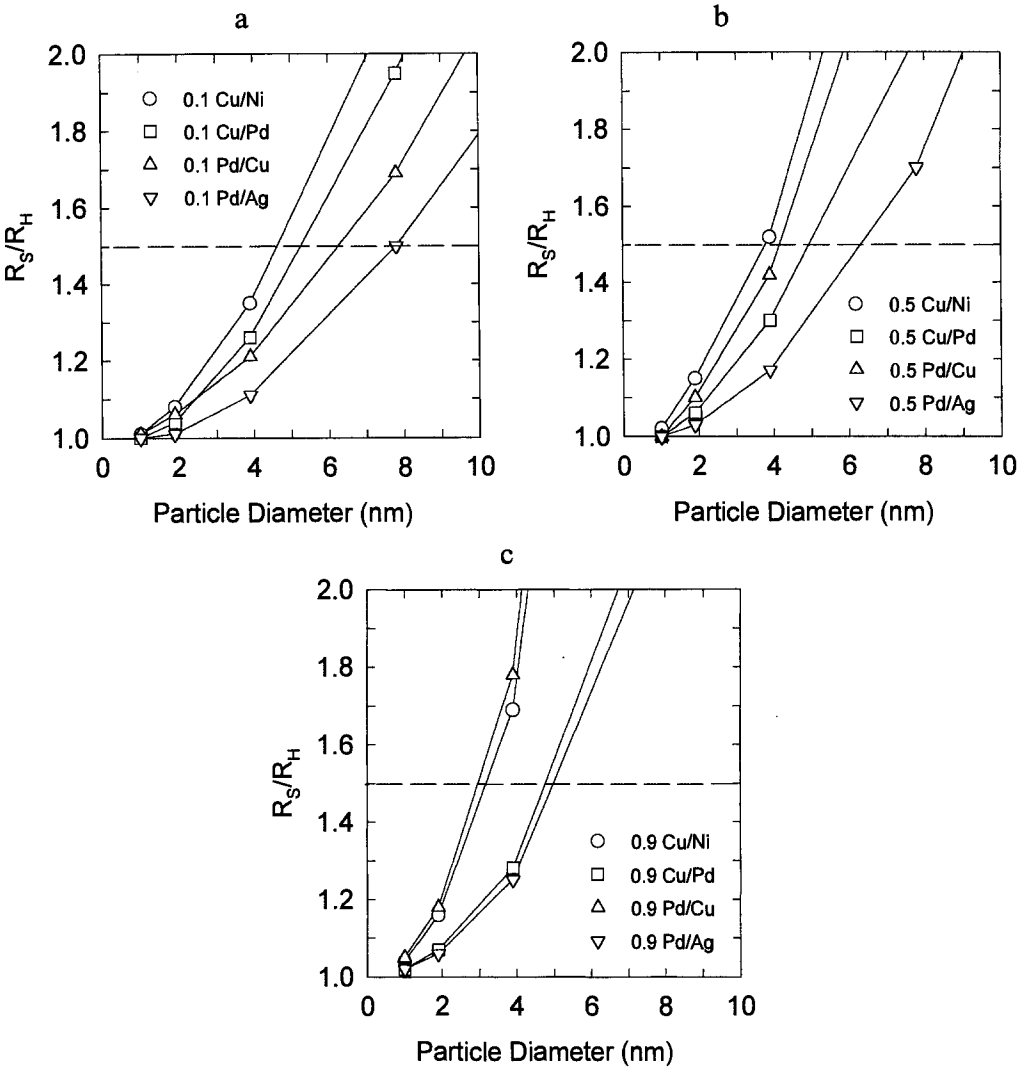

Fig. 2. R_s/R_h as a function of particle size for various metal pairs containing (a) 10%; (b) 50%; (c) 90% of the segregating metal.

ied. In general, however, discrimination between a homogeneous particle and a segregated particle becomes easier as the AL's of both metal photoelectrons decrease, as expected. Thus, in order to enhance the detection of segregation, one should use the lowest kinetic energy photoelectrons that can be reliably measured and for which accurate sensitivity factors are available. This criterion implies that Mg Kα radiation is preferred over the higher energy Al Kα radiation, in the absence of other considerations. In the case of Cu and Ni the $2p_{3/2}$ photoelectron peaks are ideal. For Pd and Ag, however, decreased AL's result from the use of $3p_{3/2}$ rather than the $3d_{5/2}$ photoelectrons considered here, but this gain is compensated by a loss in sensitivity [26].

The model predictions are validated by comparison with the limited number of experimental studies that report both XPS signal ratios and particle sizes for bimetallic particles. Glavee et al. [16] report detecting only Li on the surface of 16 nm Li–Fe particles, while Tan et al. [6] report surface enrichment of Co on Fe–Co particles without directly specifying particle size, although they describe similar pure Fe particles as "large" and covered with a "thin oxide layer, perhaps 10–20 Å thick," implying particle diameters of many nanometers. Thus, for particle diameters greater than 8 nm, XPS easily detects segregation, as predicted. In contrast, Wong et al. [14] report that XPS is inconclusive regarding surface segregation in $\sim$ 2 nm Rh–Ir particles. This result is predicted by the model since both Rh 3d and Ir 4d photoelectrons have long AL's, and this system therefore resembles the Pd/Ag system of fig. 1d that predicts a minimum particle size of 5–8 nm for detection of segregation. Of more interest are reports of XPS results for bimetallic particles within the range of 3–8 nm, where the critical particle sizes occur. Chakrabaty et al. [15] report segregation of Pt to the surface of 5.3 nm Pt–Ru particles containing 20 at% Pt. (Although particle size was not explicitly reported, the measured dispersion of 27.6% allows calculation of the particle diameter using $d = 6a/D$, where a is the metallic radius and D is the dispersion.) The measured XPS ratio is only 25% greater than expected for a homogeneous alloy, however, so the conclusion of segregation is questionable based on the criteria presented here. In terms of AL's, the Pt/Ru system most closely resembles the Pd/Ag system of fig. 1d. For Ru rich particles, one would therefore predict a minimum particle size of 6–7 nm for detection of segregation, slightly higher than the experimental particle size of 5.3 nm, and therefore consistent with the small observed enhancement in the XPS ratio. Juszczyk et al. [17] report surface segregation of Pd in Pd–Co particles for Pd–Co particles containing 25, 50, and 75% Pd, with particle diameters of 2.3, 3.7, and 8.0 nm, respectively. Comparison to fig. 1c for the very similar (in terms of photoelectron AL's) Pd/Cu system shows that the experimental particle sizes are near the predicted critical particle sizes for all compositions, and observation of surface segregation should be just possible. Note, however, that Juszczyk et al. compared bulk particle compositions to measured XPS peak area ratios corrected by the sensitivity factors of Wagner et al. [26], a method that does not account for differences in photoelectron AL's. The longer AL of Pd 3d relative to Co 2p photoelectrons would result in corrected Pd/Co XPS ratios for homogeneous particles that are higher than the bulk atomic ratios, thereby decreasing the observed enhancement attributed to Pd segregation. This effect could explain why the reported factor of two difference between the corrected XPS ratios and the bulk composition is so much greater than predicted from the model. (This explanation does not apply to the earlier mentioned studies [6,14,15] even though similar quantitation methods were used, since in each of those cases the two metals generate photoelectrons with similar AL's.)

The results presented here are significant for studies of bimetallic catalysts since the particle sizes of interest in catalysis are often in the range of 1–10 nm. Within

this size regime significant changes in particle surface morphology occur, giving rise to structure sensitivity in certain catalytic reactions [30]. The present results demonstrate that surface analytical techniques such as XPS may be unable to provide unambiguous information on surface composition for this particle size range, particularly in cases where only partial segregation occurs. Furthermore, in a supported catalyst one must account for attenuation of the XPS signals as the metal photoelectrons pass through the support material [31], adding an additional computational uncertainty to the calculations presented above. Finally, the presence of a support could influence segregation behavior, resulting in preferential segregation of one component to the interface between the support and the particle, rather than the uniform segregation assumed in the model. For all of these reasons, analysis of surface segregation in supported alloy particles by XPS or AES is questionable for particles smaller than 8 nm. Thus, XPS or AES studies claiming to detect preferential segregation in small alloy particles, without accompanying information on particle size and an appropriate analysis of the expected theoretical XPS intensity ratios, must be viewed with suspicion. The common practice of estimating surface composition in bimetallic particles using the approximate relation

$$X_{M_1} = \frac{I_{M_1}/I^{\infty}_{M_1}}{I_{M_1}/I^{\infty}_{M_1} + I_{M_2}/I^{\infty}_{M_2}} \tag{7}$$

is inadequate even for large particles since it accounts for neither the different AL's of the photoelectrons from the two metals, nor the differences between a_M and a_P.

4. Conclusions

Theoretical calculations of XPS intensity ratios for bimetallic particles show that detection of preferential surface enrichment of one of the metals is difficult for particle sizes below 8 nm, although in ideal cases detection may be possible for particles as small as 3 nm. These ideal cases consist of systems in which complete segregation occurs, the mole fraction of the segregating metal in the particle is high, and both metal photoelectrons have low kinetic energies and therefore short AL's. Detection can also be enhanced by measurement of XPS sensitivity factors on the same instrument used to analyze the bimetallic particles, rather than by relying on published sensitivity factors. Reports of surface segregation detected by XPS must therefore be viewed with suspicion unless independent particle size data is available that shows that the particles are larger than ~ 8 nm in diameter. For smaller bimetallic particles, alternative explanations for measured XPS ratios that deviate from calculated values should be sought before concluding that surface enrichment is occurring.

References

[1] J. Schwank, in: *New Trends in CO Activation*, ed. L. Guczi (Elsevier, Amsterdam, 1991) p. 225.
[2] J.H. Sinfelt, *Bimetallic Catalysts – Discoveries, Concepts and Applications* (Wiley, New York, 1983).
[3] B.C. Gates, J.R. Katzer and G.C.A. Schuit, *Chemistry of Catalytic Processes* (McGraw-Hill, New York, 1979) pp. 213ff.
[4] A. Zangwill, *Physics at Surfaces* (Cambridge University Press, New York, 1988) pp. 85, 86.
[5] E. Iglesia, S.L. Soled, R.A. Fiato and H.V. Grayson, J. Catal. 143 (1993) 345.
[6] B.J. Tan, K.J. Klabunde and P.M.A. Sherwood, Chem. Mater. 2 (1990) 186.
[7] J.W. Bassi, F. Garbassi, G. Vlaic, A. Marzi, G.R. Tauszik, G. Cocco, S. Galvagno and J. Schwank, J. Catal. 64 (1980) 405.
[8] S. Galvagno, J. Schwank, G. Parravano, F. Garbassi, A. Marzi and G.R. Tauszik, J. Catal. 69 (1981) 283.
[9] I.E. Wachs, D.J. Dwyer and E. Iglesia, Appl. Catal. 12 (1984) 201.
[10] P.C. Liao, J.J. Carberry, T.H. Fleisch and E.E. Wolf, J. Catal. 74 (1982) 307.
[11] P.C. Liao, T.H. Fleisch and E.E. Wolf, J. Catal. 75 (1982) 396.
[12] Z. Zsoldos, T. Hoffer and L. Guczi, J. Phys. Chem. 95 (1991) 798.
[13] K. Balakrishnan and J. Schwank, J. Catal. 127 (1991) 287.
[14] T.C. Wong, L.F. Brown and G.L. Haller, J. Chem. Soc. Faraday Trans. I 71 (1981) 519.
[15] D.K. Chakrabarty, K.M. Rao, A.A. Desai and P. Basu, in: *Advances in Catalysis Science and Technology*, ed. T.S.R. Prasada Rao (Wiley, New York, 1985) p. 199.
[16] G.N. Glavee, C.F. Kernizan, K.J. Klabunde, C.M. Sorenson and G.C. Hadjapanayis, Chem. Mater. 3 (1991) 967.
[17] W. Juszczyk, Z. Karpinski, D. Lomot, J. Pielaszek, Z. Paál and A.Yu. Stakheev, J. Catal. 142 (1993) 617.
[18] M.P. Seah and W.A. Dench, Surf. Interf. Anal. 1 (1979) 2.
[19] R.F. Reilman, A. Msezane and S.T. Manson, J. Electron Spectry. 8 (1976) 389.
[20] M.P. Seah, in: *Practical Surface Analysis by Auger and X-ray Photoelectron Spectroscopy*, eds. D. Briggs and M.P. Seah (Wiley, New York, 1983) pp. 182ff.
[21] S. Ichimura and R. Shimizu, Surf. Sci. 112 (1981) 386.
[22] A.G. Sault and D.W. Goodman, in: *Molecule Surface Interactions*, ed. K.P. Lawley (Wiley, New York, 1989) p. 153.
[23] S. Tanuma, C.J. Powell and D.R. Penn, Surf. Sci. 192 (1987) L849.
[24] B. Lesiak, A. Jablonski, Z. Prussak and P. Mrozek, Surf. Sci. 223 (1989) 213.
[25] C.J. Powell, J. Electron. Spectry. 47 (1988) 197.
[26] C.D. Wagner, L.E. Davis, M.V. Zeller, J.A. Taylor, R.M. Raymond and L.H. Gale, Surf. Interf. Anal. 3 (1981) 211.
[27] C.D. Wagner, W.M. Riggs, L.E. Davis, J.F. Moulder and G.E. Muilenberg, *Handbook of X-ray Photoelectron Spectroscopy* (Perkin-Elmer Corp., Eden Prairie, 1979).
[28] M.P. Seah, Surf. Interf. Anal. 2 (1980) 222.
[29] T.B. Massalski, *Binary Alloy Phase Diagrams*, 2nd Ed. (ASM International, Materials Park, 1990).
[30] M. Boudart, Adv. Catal. 20 (1969) 153.
[31] F.P.J.M. Kerkhof and J.A. Moulijn, J. Phys. Chem. 83 (1979) 1612.